Experimental studies of the *ortho*-toluidine glass transition

G. Pratesi,[1] P. Bartolini,[1,2] D. Senatra,[1,3] M. Ricci,[2,4] R. Righini,[1,2,5] F. Barocchi,[1,3] and R. Torre[1,2,3]
[1]*INFM (Instituto Nazionale per la Fisica della Materia), UdR di Firenze, Polo Scientifico, G. Sansone 1, I-50019 Sesto, Firenze, Italy*
[2]*LENS (Laboratorio Europeo di Spettroscopia Non Lineare), Polo Scientifico, via Carrara 1, I-50019 Sesto, Firenze, Italy*
[3]*Dipartimento di Fisica, Università di Firenze, Polo Scientifico, G. Sansone 1, I-50019 Sesto, Firenze, Italy*
[4]*Dipartimento di Chimica, Università della Basilicata, via N. Sauro 85, I-85100 Potenza, Italy*
[5]*Dipartimento di Chimica, Università di Firenze, Polo Scientifico, via Della Lastruccia 3, I-50019 Sesto, Firenze, Italy*
(Received 26 June 2002; published 26 February 2003)

The thermodynamic and dynamics proprieties of *ortho*-toluidine, in the vicinity of a glass transition, have been studied by calorimetric and by two light scattering techniques, depolarized light scattering and time-resolved optical Kerr effect. Differential scanning microcalorimetry clearly detects a glass transition in *o*-toluidine and it measures some thermodynamics critical parameters, in particular, the transition temperature. The light scattering data have been analyzed according to the mode-coupling theory. This theory gives a good interpretation of our data and it allows to extract safely the critical parameters of the *o*-toluidine dynamics. We found a fair agreement between the analysis outputs performed in the frequency domain and in the time domain. Finally, we compared the glass transition features of *o*-toluidine with that of its isomer *meta*-toluidine, looking for some general idea about the molecular aspects of the glass transition.

DOI: 10.1103/PhysRevE.67.021505 PACS number(s): 64.70.Pf, 78.35.+c, 61.12.−q

I. INTRODUCTION

The physics of the glass transition has received great attention during recent years, whether from the experimental or the theoretical point of view. Despite the impressive development of glass-former physics, it is substantially unknown which molecular characteristics drive a liquid phase to form a glass or a crystal and how they modify the thermodynamic and dynamic features of the transition. These problems are of fundamental importance and they deserve to be carefully considered. Indeed, many different physical parameters contribute to define how a liquid changes its proprieties during the cooling down, and then, eventually, how it forms an amorphous phase avoiding crystal nucleation. The interplay of all these parameters makes this problem very complex, for a review see [1,2].

The molecular interactions are definitely a key parameter and their role in the transition characteristics has not been elucidated. As a first approximation, two principal features of the intermolecular potential can be considered: the strength and the steric character of the interaction. From the experimental point of view, interesting information on the influences of these two features on the transition nature can be studied, in a selective way, measuring the thermodynamic and dynamic characteristics of the transition on a particular series of molecules.

Interesting studies have been worked out, recently, by Alba-Simionesco *et al.* performing a detailed thermodynamic study on a series of meta isomers which show large differences in the inter-molecular interaction strength [3,4]. All these meta isomers, which have the same molecular conformation, easily form a glass, but the temperature of transition and the calorimetric features are strongly affected by the strength and nature of the molecular interaction. In the present work we want to focus on a different aspect of the problem: how the steric characteristics of the molecular structure modify the transition features. In this framework, the three isomers (ortho, meta, and para) of a disubstituted benzene ring compound (toluidine) are interesting samples, because they have very similar strengths of molecular interaction but quite different molecular conformations, which result in different directional proprieties of the intermolecular potential. In Fig. 1 we report the three different shapes of these isomers (*o*-toluidine, *m*-toluidine, and *p*-toluidine) that differ from one another in the relative position in the benzene ring of the amino group, NH_2, with respect to the CH_3

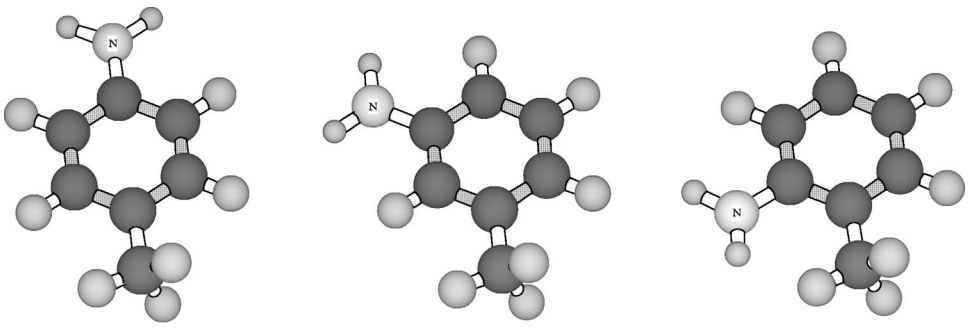

FIG. 1. The molecular structure of the three isomers: (a) *para*-toluidine, (b) *meta*-toluidine, and (c) *ortho*-toluidine. The isomers differ in the position of the NH_2 group with respect to the CH_3 group. This is position 4 for *p*-toluidine, 3 for *m*-toluidine, and 2 for *o*-toluidine.

 ©2003 The American Physical Society

group. These three isomers show very different behaviors *m*-toluidine forms a glass very easily, while *o*-toluidine and *p*-toluidine were not considered to be glass-forming materials [3], at least for a standard cooling rate. Indeed we found *p*-toluidine not able to produce a glass, even for a very fast cooling rate, whereas *o*-toluidine will be demonstrated here to have a glass transition, though it is less easy to realize then *m*-toluidine.

The previous considerations make it, therefore, interesting to study the thermodynamic and dynamic proprieties of *o*-toluidine in the liquid states approaching the supercooled phase and possibly the glass transition. We first measured the thermodynamic properties of *o*-toluidine, detecting a clear glass transition, then we investigated its dynamical behavior by two light scattering experiments: depolarized light scattering (DLS) [5–7] and the time-resolved optical Kerr effect (OKE) [8–11]. We compared our light scattering results with the mode-coupling theory (MCT) predictions [12,13], in order to verify the MCT predictions and to extract the glass transition parameters. Furthermore, we compare the *o*-toluidine transition parameters with those characterizing *m*-toluidine, obtained by previous thermodynamic [4] and dynamic [6,9,10] measurements.

In this paper Sec. II is devoted to the presentation of the results of the differential scanning micro-calorimetry (DSC) for the determination of T_g in *o*-toluidine, Sec. III gives the experimental results and the analysis of the DLS spectra at various temperatures, Sec. IV gives the experimental results of the OKE measurements and analysis, Sec. V gives the conclusion.

II. DIFFERENTIAL SCANNING MICRO-CALORIMETRY

All experiments reported in this paper have been performed on liquid *o*-toluidine (99%) purchased from Merck and subsequently purified by differential distillation in our laboratory. The thermal behavior of *o*-toluidine was investigated in the temperature range from 293 K down to 103 K. The glass transition of the above liquid was witnessed both during the freezing of the liquid sample and the heating of the vitrified one.

The study was performed with a Mettler TA 3000 heat flux differential scanning microcalorimeter equipped with a TC 10A processor and a low temperature cell, model DSC 30 Silver. The equipment was modified in order to allow the refilling of the liquid nitrogen Dewar without removing the low temperature cell, while the instrument is kept on in a given standby state. In this way the calibration assessment of the measuring head is maintained constant over long lasting measuring runs. Aluminum pans were used for both the reference and the sample. The sample mass was measured with a MX5 Mettler Toledo microbalance with an accuracy of ± 1 μg. After each measuring run, the sample mass was checked in order to exclude any leakage during the measure. The effect of the different thermal rates dT/dt of 2, 4, and 10 K/min was tested. Depending on the thermal rate applied, the temperature accuracy was of ± 0.2, ± 0.3, and ± 0.5 K, respectively. To compensate for contributions to the specific heat c_p in J/gK, arising from a difference in weight between the pan used as the reference and the one filled with the sample, each measuring run was preceded by a blank experiment with the same reference pan and the sample pan, with its lid, empty and unsealed. The results of the blank procedure were recorded. Thereafter, the final measuring run was carried out by applying the same experimental conditions adopted in the blank experiment with always the same reference crucible and with the sample holder pan filled with the system under test. The above procedure was of paramount importance in the evaluation of the glass transition parameters as well as in the analysis of c_p as a function of temperature. Greater details about both the instrument and the measuring procedures adopted in the thermal analysis can be found in Refs. [14,15].

The parameter dH/dt, where H is the enthalpy, could be measured within the range of 17 mW, using the highest instrumental sensitivity. We recall that, for condensed systems at constant pressure, the heat change δQ is equal to the enthalpy change δH for any thermal transition. The enthalpy values δH in J/g, at constant pressure, associated with the melting process of the *o*- and *m*-toluidine, were evaluated with the thermal rate of 2 K/min, because with the latter thermal rate the base lines for the integration of the melting peaks of the two liquids, are much better defined than with the 10 K/min rate. The melting temperatures were evaluated with the Onset method to detect the intersection point of the evaluated regression line with the experimentally recorded baseline as well as the tangent to the experimental curve inflection point. For the glass transition three temperatures were evaluated, namely, T_1 at the intersection of the regression line from the start with the inflection tangent of the glass transition "step," T_2 at the point where the transition of the sample is 50% complete and T_3 at the intersection of the inflection tangent with the regression line after the transition itself. Regression lines were computed before and after the glass transition, each one over 45 measuring points (seconds). The description *in extenso* of the thermal analysis of *o*-toluidine will be reported elsewhere.

The trend of c_p as a function of decreasing temperature at the glass transition, is reported in Fig. 2 for both *o*- and *m*-toluidine. The same analysis performed upon heating the vitrified samples gave substantially the same results but for a shift to slightly lower values of the glass transition temperatures.

The glass transition parameters for both *o*- and *m*-toluidine are reported in Table I for the thermal rates of 2 and 10 K/min, *m*-toluidine was used as reference system. For the sake of completeness, the enthalpy values associated with the melting of both samples were also calculated from the NSC spectra [14,15] collected by heating samples with a thermal rate of 2 K/min. The calculated values are: $\delta H = 71.2$ J/g for *o*-toluidine and $\delta H = 82.5$ J/g for *m*-toluidine. The melting temperatures were $T_m = 249.5$ K and 242.2 K, respectively. As often reported in literature, the temperature T_2 can be taken as the glass transition temperature. According to the present analysis we found a value of $T_g \sim 189$ K for *o*-toluidine and a value of $T_g \sim 188$ K for *m*-toluidine, in agreement with the literature value $T_g = 187$ K [4]. Indeed the thermodynamic behavior of these two isomers at the

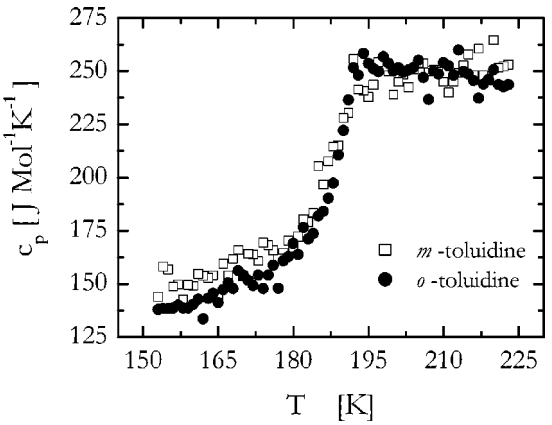

FIG. 2. c_p behavior as a function of decreasing temperature at the glass transition.

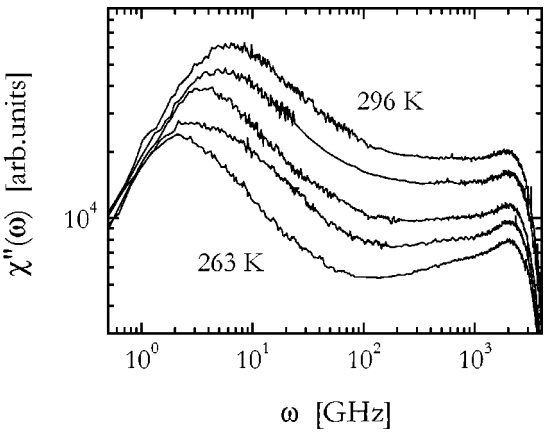

FIG. 3. Susceptibility DLS spectra. From the top the temperatures are 296, 288, 281, 274, and 263 K, respectively. The intensity spectra are shifted in order to a avoid a crowded picture.

glass transition is substantially identical as can be seen clearly from the c_p temperature dependence, see Fig. 2. These results also confirm how these two isomers have very similar intermolecular strengths. In fact, it has been proved that a small variation in the intermolecular strengths produces a sensible modification of the glass transition temperature [4].

III. DEPOLARIZED LIGHT SCATTERING

The depolarized light scattering spectra of *o*-toluidine have been measured at five temperatures: 296, 288, 281, 274, and 263 K, at 1 bar pressure. The sample is kept in a thermostated optical quartz cell and the temperature controlled with an accuracy of 0.5 K by means of a thermocouple inserted in the body of the scattering cell. The spectra were excited with an ion argon laser source at a wavelength of 488 nm, intensity 200 mW, and collected at 90° scattering geometry in a depolarized configuration. The scattering signal is measured by photon counting detection. The scattered light spectrum was analyzed between -30 and 4000 GHz by means of a high resolution Raman double monochromator, SOPRA DMDPM2000, with a maximum frequency resolution of 1 GHz [7].

In Fig. 3 we show the susceptibility spectra recorded at different temperatures. The susceptibility is obtained according to the following equation:

$$\chi''(\omega) = \frac{I_{VH}(\omega)}{[n(\omega)+1]}, \tag{1}$$

where $I_{VH}(\omega)$ is the depolarized spectrum intensity and $n(\omega)$ is the Bose-Einstein factor. It is easy to see that, as the temperature decreases, the α peak shifts toward lower frequency, while the minimum in the spectra becomes deeper, as is usually expected. We analyze the spectral data within the framework of the MCT. According to the MCT the system dynamics is characterized by two main time regimes: the slow dynamics, also called the α regime, and a faster one, called the β regime. Under the appropriate approximation this theory predicts that the correlation function of the relevant physical observable decays in the α regime as the Kohlrausch-Williams-Watts (KWW) or stretched exponential function. In order to fit the lower frequency region of spectra,

TABLE I. Thermal analysis of the glass transition of *ortho*- and *meta*-toluidine.

ortho-toluidine						
Thermal rate	10 (K/min) upon heating			10 (K/min) upon freezing		
Glass trans. temperature	T_1	T_2	T_3	T_1	T_2	T_3
	189	191	193	192	187	182.5
Thermal rate	2 (K/min) upon heating			2 (K/min) upon freezing		
Glass trans. temperature	T_1	T_2	T_3	T_1	T_2	T_3
	187	189.5	192	193.5	188	182
meta-toluidine						
Thermal rate	10 (K/min) upon heating			10 (K/min) upon freezing		
Glass trans. temperature	T_1	T_2	T_3	T_1	T_2	T_3
	189	192	193	190.5	186	182
Thermal rate	2 (K/min) upon heating			2 (K/min) upon freezing		
Glass trans. temperature	T_1	T_2	T_3	T_1	T_2	T_3
	187	188.5	191	191	186	181

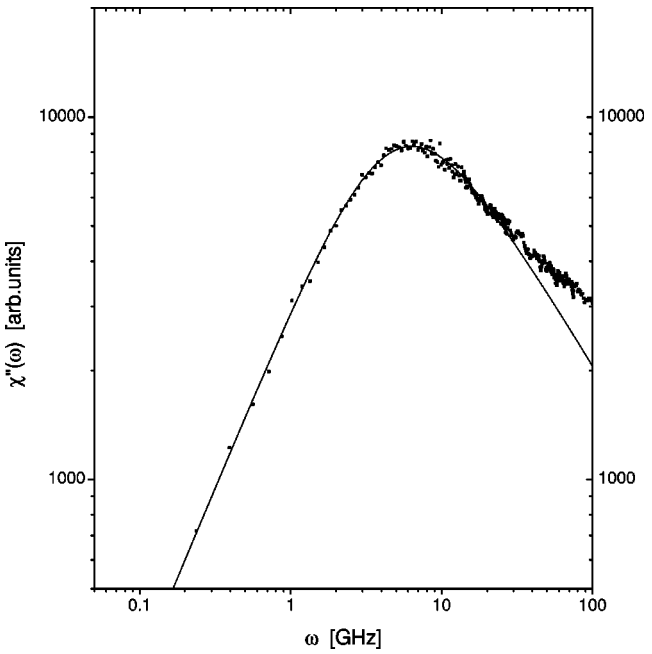

FIG. 4. Fit of $\chi''(\omega)$ in the α region for the spectra at $T=296$ K according to Eq. (2).

which corresponds to the α regime, we should use an analytical Laplace transform of this time dependent function. Unfortunately this function cannot be analytically transformed but it can be well approximated by the Cole-Davidson expression [16]:

$$\chi_{CD}(\omega)=\frac{\chi_0}{(1+i\omega\tau_{CD})^{\beta_{CD}}}, \tag{2}$$

where the Cole-Davidson relaxation time τ_{CD} and stretched exponential β_{CD} are related to the Kohlrausch relaxation time τ_K and stretching exponent β_K through the following linear relation [16]:

$$\begin{aligned}\tau_K&=\tau_{CD}(1.184\beta_{CD}-0.184),\\ \beta_K&=0.683\beta_{CD}+0.316.\end{aligned} \tag{3}$$

We have fitted the α-relaxation part of the spectra with the imaginary part of the Cole-Davidson function convoluted with the instrumental response of our apparatus. A typical fit is shown in Fig. 4 and Table II gives the value of the β_K and τ_K obtained from the fit and from expression (3).

According to the MCT, the faster region of the spectra, also called the β-relaxation region, where a minimum is present, can be properly reproduced by the following interpolation formula [5,12,13]:

$$\chi''(\omega)\propto b(\omega/\omega_{min})^a+a(\omega_{min}/\omega)^b, \tag{4}$$

which is a good approximation in the region of the minimum, with the parameters a and b related by [12]

$$\lambda=\Gamma^2(1-a)/\Gamma(1-2a)=\Gamma^2(1+b)/\Gamma(1+2b), \tag{5}$$

where λ is the MCT "exponent parameter" and Γ is the Euler function. In the end, using Eq. (4) and the constrain

TABLE II. τ_α and β values obatined from the analysis of the α part of the DLS spectra.

Temperature (K)	β_K	τ_K (ps)
296.7	0.73	26.2
288.1	0.69	33.7
281.1	0.71	43.4
274.1	0.72	56.6
263.1	0.73	78.6

condition stated by Eq. (5), the fitting procedure has only two free parameters: a and χ''_{min}, a being a parameter independent of temperature. From the best fit we found the χ''_{min} parameters, reported in Fig. 6(b), and $\langle a\rangle=0.33\pm0.02$ [hence $b=0.65\pm0.1$ as obtained by Eq. (5)]. Finally we derive the value of the MCT critical exponent $\gamma=1/2a+1/2b$, which is $\gamma=2.28\pm0.2$. In Fig. 5 we show a master plot of the susceptibility together with the masterfit of the β-relaxation region. We found the MCT rescaling procedure applicable and the master-fit parameters turn out to be in very good agreement with the previous fitting analysis.

Following the MCT scaling laws, τ_K, χ''_{min}, and ω_{min} should depend on temperature as [12,13]:

$$\tau_K^{-1/\gamma}\propto(T-T_C), \tag{6}$$

$$(\chi''_{min})^2\propto(T-T_C), \tag{7}$$

$$\omega_{min}^{2a}\propto(T-T_C). \tag{8}$$

In Fig. 6(a) the dependence of $\tau_K^{-1/\gamma}$ on the temperature is shown while in Fig. 6(b) the dependence of $(\chi''_{min})^2$ and ω_{min}^{2a} are shown. The expected MCT scaling laws are verified, as proved by the data linear temperature dependences. Furthermore, a linear fit of the data according to Eqs. (6)–(8), respectively, leads to the same critical temperature, within the experimental errors. The mean value is $T_C=215\pm10$ K. So we found that the MCT predictions describe properly our DLS data on *o*-toluidine. Moreover, the MCT

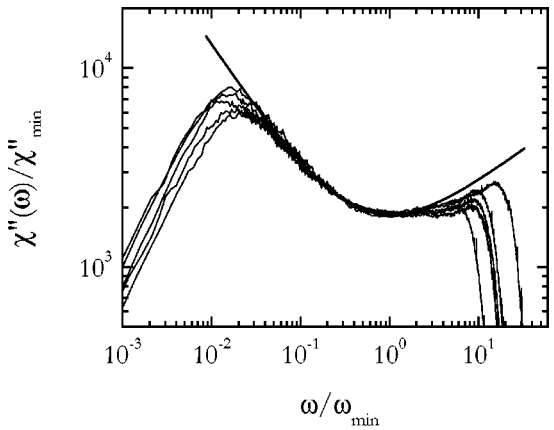

FIG. 5. Master plot of the susceptibility for the β region together with the fit using Eq. (4).

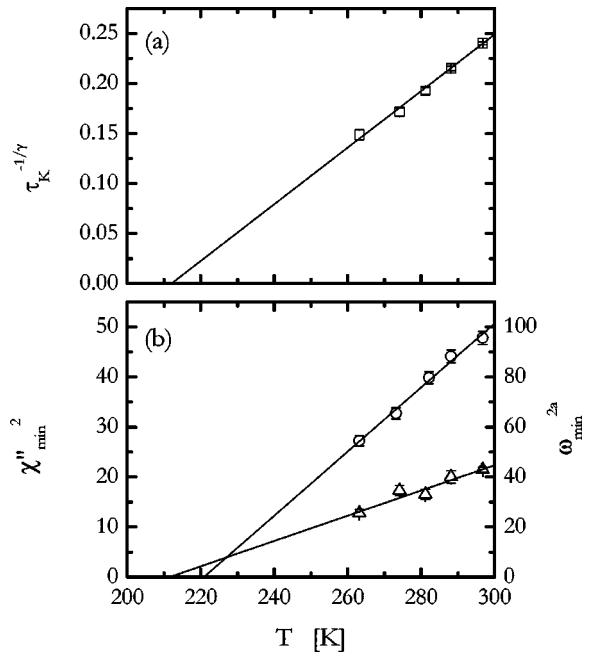

FIG. 6. (a) Dependence of $\tau_K^{-1/\gamma}$ (open square) on the temperature, the straight line is a fit using Eq. (6). (b) Dependence of $(\chi''_{\min})^2$ (open circle) and ω_{min}^{2a} (open triangle) on the temperature with a fit according to Eqs. (7) and (8), respectively.

data analysis applied to two independent frequency regions of the spectra, α and β-region, gives consistent values of the critical temperatures.

A comparison with the dynamical proprieties of *m*-toluidine is necessary. The MCT parameters of *o*-toluidine have substantially the same values as the *m*-toluidine parameters measured in a previous DLS experiment [6]. These agreements suggest that the dynamics of the present isomers, in the proximity of a glass transition, is not strongly affected by the directional characteristic of the intermolecular potential.

IV. OPTICAL KERR EFFECT

In transient OKE experiments an excitation polarized laser pulse induces an optical birefringence in the sample, then the relaxation of this anisotropy toward the equilibrium is probed through the change of polarization of a second pulse. Increasing the temporal delay between pump and probe pulses, it is possible to detect the relaxation of the induced birefringence directly in the time domain. In our experiment we perform a heterodyne detection with an apparatus that has been already described in a previous paper [17]. The heterodyne detected OKE (HD-OKE) signal $S(t)$ is given by the convolution of the second-order pulse intensity autocorrelation with the material response function $R(t)$. When the pulse duration is short compared to the characteristic relaxation time of the response function, we can neglect the convolution and so we have $S(t) \propto R(t)$. According to the linear response theory, the response function $R(t)$ is directly related to the correlation function of the dielectric tensor of the material [18,19]. So the OKE experiment measures, directly in the time domain, the same dynamical information obtained by the DLS experiment [20].

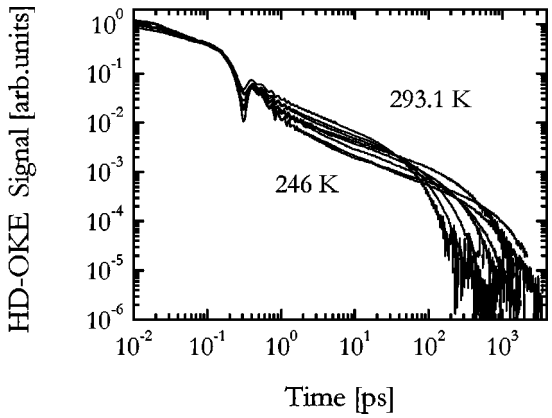

FIG. 7. HD-OKE signal for $T = 293.1$, 283.6, 273.4, 262.9, 258, 255.7, 248.7, 246 K.

The optical experimental setup has been described in detail elsewhere [17]. The laser system consists of a Kerr-lens mode-locking Ti:sapphire oscillator (20 fs pulse duration) and a Nd:YLF laser pumped Ti:sapphire regenerative amplifier (1 KHz repetition rate). In order to extend the experimental temporal range, we measured the slow part of the decay using a 1-ps stretched pulse with 12 μJ of energy and the fast part using a 50 fs transform limited pulse with 1.2 μJ [21,22].

The HD-OKE data on the *o*-toluidine sample are collected at different temperatures from 246 K to 293 K. The sample was kept in a quartz cell of 2 mm optical path and the cell was placed in an homemade Peltier cryostat with a temperature accuracy of ± 0.5 K. The HD-OKE measurements are shown in Fig. 7. These data can be divided into three temporal regions: the very fast time window (0–300 fs) is characterized by a temperature-independent electronic response, the fast and intermediate region (0.3–30 ps) is characterized by a weak temperature dependence, and finally the slow response (0.03–4 ns), where the signal exhibits a slow relaxation, is characterized by a strong temperature dependence. In the fast time region (0.3–2 ps) the signal shows an oscillating dynamics addressed to intramolecular vibrations that are coherently excited by the pump laser pulse.

As for the DLS data, we analyzed the OKE data with the support of the MCT. In the present study, we investigated the slow part of the decay corresponding to the MCT α-relaxation region and the intermediate decay related to the late part of β relaxation, also called the von Schweidler (VS) region [12,13]. First of all, we test the time-temperature superposition-principle [10,12]. In Fig. 8 we show the master-plot obtained by rescaling the time and amplitude axes. This method provided a set of rescaling time values τ_α and amplitude values χ_α without using any specific fitting function. The time and amplitude values are reported in Table III. Then, we checked the decay functions predicted by the MCT. As we introduced previously, the HD-OKE signal is directly proportional to the sample response function $R(t)$. This response is again proportional to the time derivative of the dielectric constant correlator function [10,19]. Therefore, the time derivative of the functional form provided by the MCT theory must be used [8,10]. So to fit the slow part of

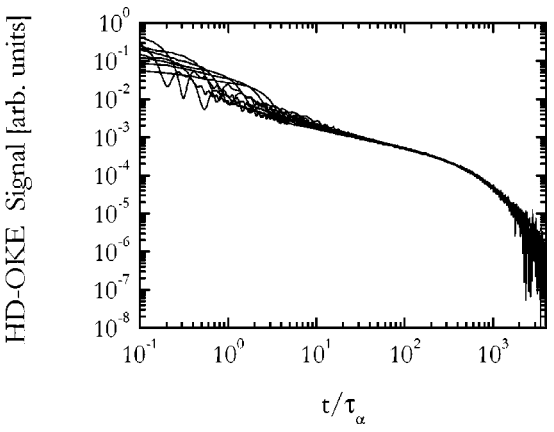

FIG. 8. Master plot of the HD-OKE data, obtained by rescaling the time and amplitude axes.

the decay, corresponding to the low frequency region or α-relaxation region, we used the time derivative of the Kohlrausch function (dKWW):

$$S(t) \propto \chi_K(T) \left[\frac{t}{\tau_K(T)} \right]^{\beta_K - 1} e^{-(t/\tau_K(T))^{\beta_K}}, \tag{9}$$

where β_K is the stretching exponential factor. This analytical function, Eq. (9), well reproduces the long part of the decay, providing a good fit over three decades. In Table III we also report the values of the time and amplitude scale factors obtained from the fittings at each temperature. The two series of values from the rescaling, τ_α and χ_α, and from the fitting procedures, τ_K and χ_K, are in very good agreement. As is explained in the previous works [8–10,22], this method is a good test of the MCT predictions, because two different analyses of the α region are used and their consistency is compared. The evaluation of the MCT parameters T_C and γ is done by analyzing the temperature dependence of τ_K and χ_K. The MCT predicts the following α-scaling laws:

$$\tau_K \propto (T - T_C)^{-\gamma}, \tag{10}$$

$$\chi_K \propto \frac{(T - T_C)^{\gamma}}{T}, \tag{11}$$

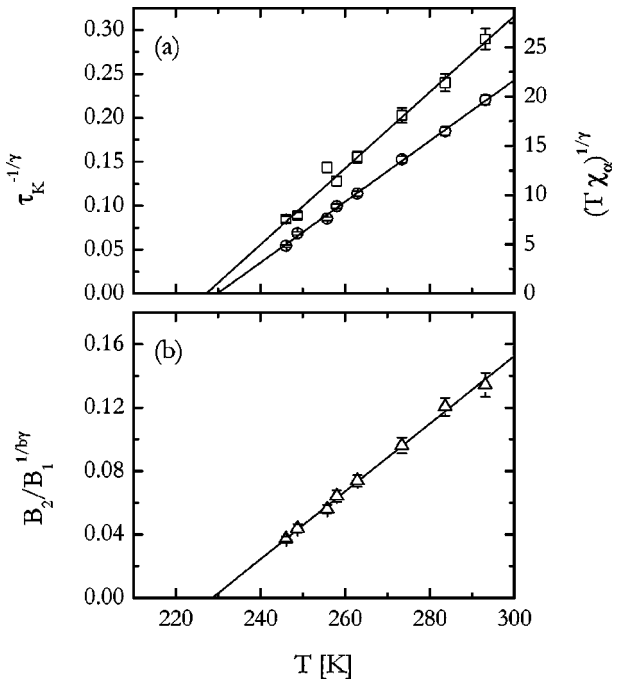

FIG. 9. (a) Linearized plot of τ_K (open square) and χ_K (open circle) vs temperature. The straight lines are fits according to Eqs. (10) and (11). The fitting parameters are $T_C = 230.2$ K, $\gamma = 2.2$, and $T_C = 227$ K, $\gamma = 2.4$, for τ_K and χ_K, respectively. (b) Linear plot of $(B_2/B_1)^{1/b}$ vs temperature. The fit is performed with Eq. (13) resulting in $T_C = 229$ K and $\gamma = 2.43$.

where Eq. (10) is equivalent to Eq. (6) previously reported. Figure 9 shows that the α-scaling laws are well verified and a good fit can be obtained with $T_C = 230 \pm 5$ K, $\gamma = 2.2 \pm 0.3$ and $T_C = 227 \pm 4$ K, $\gamma = 2.4 \pm 0.1$, according to Eqs. (10) and (11), respectively.

According to the MCT, the intermediate relaxation, or VS region, equivalent to the slow part of the minimum in a frequency spectra, can be properly reproduced by the VS decay function [5,12,13]. So we fitted the OKE signal, in the intermediate time-region, with the derivative of such a function:

$$S(t) \propto B_1 t^{b-1} + B_2 t^{2b-1}, \tag{12}$$

where the next to leading order correction has been intro-

TABLE III. Values of the fitting parameters related to the α-region from the master-plot analysis (second and third columns) and from the dKWW analysis (fourth, fifth, and sixth columns). The τ_α and χ_α are normalized on the values of τ_K and χ_K at the lowest temperature. In the last three columns, the fitting results of the VS region are reported.

Temp. (K)	τ_α (ps)	χ_α (a.u.)	τ_K (ps)	χ_K (a.u.)	β_K	B_1 (a.u.)	B_2 (a.u.)	b
293.1	27±5%	8.8±10%	27±5%	8.4±10%	0.82±4%	28±2	2.5±0.4	0.52±5.5%
283.6	37	5.9	39	5.5	0.83	20±1	1.2±0.2	0.56
273.4	60	3.8	59	3.8	0.78	16±1.2	0.8±0.1	0.55
262.9	110	2.1	112	2.1	0.79	12.1±0.6	0.4±0.05	0.55
258.0	155	2.5	150	1.3	0.76	9.5±0.7	0.31±0.05	0.53
255.7	212	1.8	209	1.8	0.74	12.8±0.6	0.3±0.003	0.56
248.7	371	0.53	337	0.58	0.74	6.1±0.6	0.13±0.03	0.53
244.5	554	0.52	554	0.52	0.78	5.5±0.4	0.07±0.01	0.56

duced [23]. The B_1/B_2 ratio is temperature dependent according to the following VS-scaling law [23]:

$$\left(\frac{B_2}{B_1}\right)^{1/b} \propto (T-T_C)^{\gamma}. \tag{13}$$

In Table III we report the fitting results for each temperature. All the b exponent fitting parameters are equal, within the error bar. The mean value is $\langle b\rangle = 0.54 \pm 0.02$ corresponding to $\gamma = 2.58 \pm 0.1$. In Fig. 9(b) we verified the VS-scaling law and fitted the experimental data according to Eq. (13). A reasonable good fit can be obtained with $T_C = 229 \pm 7$ K and $\gamma = 2.34 \pm 0.3$, which are, within the error bars, in agreement with the values found by the previous analyses.

Definitely, the time-resolved OKE experiment gives a very good insight of the relatively slow relaxation of this glass former, yielding a measure of the α-relaxation times affected by a small uncertainty. Furthermore, the OKE data allow an articulated and nontrivial check of the MCT scenario. The present *o*-toluidine data support the MCT interpretation of the glass transition, nevertheless a complete check should extend over a wider range of temperatures including that in the vicinity of T_C. The *o*-toluidine MCT parameters, found with the OKE investigation, are in fair agreement with the DLS results presented in Sec. II; furthermore, they substantially coincide with the *m*-toluidine parameters obtained in a previous work [10]. Again, our experimental data suggest that the dynamics of these two toluidine isomers are not strongly affected by the different molecular structures.

V. CONCLUSION

The paper reports on the experimental characterization of an important glass former: *o*-toluidine. We investigated the thermodynamic and dynamic proprieties of this glass former and compared them with those of *m*-toluidine.

According to the differential scanning microcalorimetry performed on both these isomers, the liquid-glass transition is characterized by nearly the same parameters; in particular, the glass transition temperatures are substantially identical for these two compounds. This result suggests that the thermodynamic proprieties, approaching the glass state, are not substantially modified by the differences in the intermolecular potential presented by these two molecular liquids.

DLS and OKE experiments allowed us to extract the dynamic parameters of the glass transition in the framework of the MCT. According to our analysis, the MCT model produces a valid interpretation of the *o*-toluidine dynamics and it gives reliable fitting parameters. A comparison of the dynamic proprieties of these two isomers, restricted to the intermediate and slow relaxation regions, shows that they are only slightly affected by the change of the molecular structure on passing from meta to ortho isomers.

On the basis of the results presented here, we can speculate some implication of the molecular structure on the glass transition features. As we noticed in Sec. I, the intermolecular potential is indeed a key feature in the competition between the nucleation and formation of an amorphous phase, and on the definition of the transition features. The strengths of the molecular interactions of the three toluidine isomers are very similar, because they are dominated by the intermolecular hydrogen bonds involving the NH_2 groups, whose strengths are not expected to change noticeably from one isomer to the other. In addition, the molecular dipole moments are very similar (1.6 D for *o*-toluidine, 1.45 D for *m*-toluidine, and 1.52 D for *p*-toluidine). So the intermolecular potential, in these isomers, differs mainly by the steric features of the molecules, and our experimental results have to be ascribed to the variation of the molecular shapes.

First of all, we found that *p*-toluidine does not show any tendency to form a glass phase, even at a very fast cooling rate. Probably the relatively high symmetry (pseudo-C_{2v}) of this isomers makes the nucleation phenomena easier, suppressing a possible glass phase. On the other hand, *o*- and *m*-toluidine can easily be cooled to a glass phase, with very similar values of the thermodynamic and dynamical parameters of the transition. It is quite striking that moving the NH_2 group from position 2 (*ortho*-) to position 3 (*meta*-), see Fig. 1, produces only minor changes in the transition features of these liquids and, on the contrary, *p*-toluidine, where the NH_2 is in position 4, behaves very differently. These experimental results show that even the pure molecular geometry can play a fundamental role in the definition of the transition nature and characteristics.

Recent experimental and numerical studies [24,25] have proved that *m*-toluidine shows a clear clustering phenomenon in the supercooled phase and that the MCT critical temperature corresponds to a variation of the clusters structure. According to these works we could suggest that the glass transition in both *o*- and *m*-toluidine isomers appears through some clustering effect and the suppression of this clustering phenomenon in *p*-toluidine, replaced by nucleation, prevent the glass formation. Furthermore, the thermodynamic and dynamic features of the *o*- and *m*-toluidine liquids approaching the transition are dominated by very similar clustering processes, so that no evident differences between these two liquids can be experimentally detected. These results suggest also some interesting observations about the energy landscape scenario [2] behind the found phenomena. Actually, the high symmetry present in the *p*-toluidine molecule strongly reduces the dimensionality of the potential energy hypersurface of the liquid, compared to that of the other two isomers, and makes it much easier for the para isomer to maintain ergodicity in its route to the crystal minimum. Presumably, the possible trajectories on the potential hypersurface along which two molecules can approach each other are remarkably higher for the two isomers of lower symmetry (*o*- and *m*-toluidine). This may lead to a clustering phenomenon and prevent the overall system from maintaining ergodicity as cooling proceeds.

ACKNOWLEDGMENTS

We thank R. Chelli, S. Califano, and M. Sampoli for very helpful suggestions and M. De Pas for the indispensable technical support. This work was supported by the Commission of the European Communities through Contract No. HPRI-CT1999-00111, by MURST cofin 2000, and by INFM.

[1] J. Wong and C.A. Angell, *Glass: Structure by Spectroscopy* (Dekker, New York, 1976); E. Donth, *The Glass Transition: Relaxation Dynamics in Liquids and Disordered Materials* (Springer-Verlag, Berlin, 2001).
[2] Pablo G. DeBenedetti, *Metastable Liquids, Concepts and Principles* (Princeton University Press, Princeton, NJ, 1996).
[3] C. Alba-Simionesco, L.E. Busse, and C.A. Angell, J. Chem. Phys. **92**, 617 (1990).
[4] C. Alba-Simionesco, J. Fan and C.A. Angell, J. Chem. Phys. **110**, 5262 (1999).
[5] H.Z. Cummins, G. Li, W. Du, Y.H. Hwang, and G.Q. Shen, Prog. Theor. Phys. Suppl. **126**, 21 (1997); G. Monaco, D. Fioretto, L. Comez, and G. Ruocco, Phys. Rev. E **63**, 061502 (2001); A. Patkowski, E.W. Fischer, W. Steffen, H. Glaser, M. Baumann, T. Ruths, and G. Meier, *ibid.* **63**, 061503 (2001).
[6] A. Aoudi, C. Dreyfus, M. Massot, R.M. Pick, T. Berger, W. Steffen, A. Patkowski, and C. Alba-Simionesco, J. Chem. Phys. **112**, 9860 (2000).
[7] G. Pratesi, A. Bellosi, and F. Barocchi, Eur. Phys. J. B **18**, 283 (2000).
[8] R. Torre, P. Bartolini, and R.M. Pick, Phys. Rev. E **57**, 1912 (1998).
[9] R. Torre, M. Ricci, P. Bartolini, C. Dreyfus, and R.M. Pick, Philos. Mag. B **79**, 1897 (1999).
[10] R. Torre, P. Bartolini, M. Ricci, and R.M. Pick, Europhys. Lett. **52**, 324 (2000).
[11] G. Hinze, D.D. Brace, S.D. Gottke, and M.D. Fayer, Phys. Rev. Lett. **84**, 2437 (2000); S.D. Gottke, D.D. Brace, G. Hinze, and M.D. Fayer, J. Phys. Chem. B **105**, 238 (2001).
[12] W. Götze and L. Sjögren, Rep. Prog. Phys. **55**, 241 (1992).
[13] W. Götze, J. Phys.: Condens. Matter **11**, A1 (1999).
[14] D. Senatra, G. Gabrielli, and G.G.T. Guarini, Europhys. Lett. **2**, 455 (1986).
[15] D. Senatra, in *Thermal Behavior of Dispersed Systems*, edited by N. Garti (Dekker, New York, 2000), Chap. VI, pp. 203–245.
[16] C.P. Lindsey and G.D. Patterson, J. Chem. Phys. **73**, 3348 (1980).
[17] P. Bartolini, M. Ricci, R. Torre, R. Righini, and I. Santa, J. Chem. Phys. **17**, 110 (1999).
[18] R.W. Hellwarth, Prog. Quantum Electron. **5**, 1 (1977).
[19] Y. Yan and K.A. Nelson, J. Chem. Phys. **87**, 6240 (1987).
[20] S. Kinoshita, Y. Kai, M. Yamaguchi, and T. Yagi, Phys. Rev. Lett. **75**, 148 (1995).
[21] M. Ricci, P. Bartolini, and R. Torre, Philos. Mag. B **82**, 541 (2002).
[22] D. Prevosto, P. Bartolini, R. Torre, M. Ricci, A. Taschin, S. Capaccioli, M. Lucchesi, and P. Rolla, Phys. Rev. E **66**, 011502 (2002).
[23] T. Franosch, M. Fuchs, W. Götze, M.R. Mayr, and A.P. Singh, Phys. Rev. E **55**, 7153 (1997).
[24] D. Morineau and C. Alba-Simionesco, J. Chem. Phys. **109**, 8494 (1998).
[25] R. Chelli, G. Cardini, P. Procacci, R. Righini, and S. Califano, J. Chem. Phys. **116**, 6205 (2002).